

Effect of different aqueous solutions on physicochemical properties of asphalt binder

Zou, Yingxue; Amirkhanian, Serji; Xu, Shi; Li, Yuanyuan; Wang, Yafei; Zhang, Jianwei

DOI

[10.1016/j.conbuildmat.2021.122810](https://doi.org/10.1016/j.conbuildmat.2021.122810)

Publication date

2021

Document Version

Final published version

Published in

Construction and Building Materials

Citation (APA)

Zou, Y., Amirkhanian, S., Xu, S., Li, Y., Wang, Y., & Zhang, J. (2021). Effect of different aqueous solutions on physicochemical properties of asphalt binder. *Construction and Building Materials*, 286, 1-12. Article 122810. <https://doi.org/10.1016/j.conbuildmat.2021.122810>

Important note

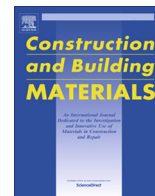
To cite this publication, please use the final published version (if applicable). Please check the document version above.

Copyright

Other than for strictly personal use, it is not permitted to download, forward or distribute the text or part of it, without the consent of the author(s) and/or copyright holder(s), unless the work is under an open content license such as Creative Commons.

Takedown policy

Please contact us and provide details if you believe this document breaches copyrights. We will remove access to the work immediately and investigate your claim.



Effect of different aqueous solutions on physicochemical properties of asphalt binder



Yingxue Zou^a, Serji Amirkhanian^b, Shi Xu^{c,*}, Yuanyuan Li^a, Yafei Wang^a, Jianwei Zhang^a

^a State Key Laboratory of Silicate Materials for Architectures, Wuhan University of Technology, Luoshi Road 122, Wuhan 430070, China

^b Department of Civil Construction and Environmental Engineering, University of Alabama, Tuscaloosa, AL 35487, United States

^c Civil Engineering and Geosciences, Delft University of Technology, Delft 2628CN, the Netherlands

HIGHLIGHTS

- Asphalt was eroded by five kinds of aqueous solutions, respectively.
- The morphology, chemical structure and four components of asphalt were observed.
- The pH, total organic carbon and chemical component of solutions were monitored.
- The oxidation, dissolution and migration of asphalt occurred alternately.
- Solute could accelerate the erosion on asphalt through interaction.

ARTICLE INFO

Article history:

Received 17 July 2020

Received in revised form 1 December 2020

Accepted 21 February 2021

Keywords:

Asphalt
Aqueous solutions
Morphology
Structure
Components

ABSTRACT

Aqueous solution is one of the main factors of asphalt pavement disease. However, the physicochemical changes of asphalt are ambiguous during immersion in different aqueous solutions. This study evaluated the physicochemical properties of asphalt under the action of different aqueous solutions to further understand the mechanism of moisture erosion. The morphology, chemical structure and four components of asphalt were observed after immersion, while the pH value, total organic carbon (TOC) and characteristic functional groups of residual solutions were monitored. The test results showed that aqueous solution could change the bee structure on the asphalt surface and increased the mean roughness. The carbonyl index ($I_{C=O}$) and sulfoxide index ($I_{S=O}$) of asphalt increased with immersion time. And the asphaltenes of asphalt fluctuated and eventually increased during immersion. Solute could accelerate the erosion on asphalt through interaction, the degree of which increased in the order, Na_2SO_4 saline < NaCl saline < pH 3 acid < pH 11 alkali.

© 2021 The Authors. Published by Elsevier Ltd. This is an open access article under the CC BY-NC-ND license (<http://creativecommons.org/licenses/by-nc-nd/4.0/>).

1. Introduction

Asphalt, an organic polymer material, is generally considered insoluble in water and less affected by water. The influence of moisture on the physicochemical properties of asphalt is often overlooked. The properties of asphalt are the main factors affecting the quality and life of asphalt pavement. The thickness of asphalt binder in asphalt pavement is only tens of microns, moisture is relatively easy to intrude into asphalt binder [1]. The moisture intrusion has a negative effect on the performance of asphalt concrete which may cause cohesion destruction of asphalt and adhesion failure between asphalt and aggregate interface [2–7]. Moreover, early damage of asphalt pavement is always related to moisture

erosion that has attracted increasing attention as a factor to accelerate the aging of asphalt in recent years [8–13]. Nevertheless, the mechanism of moisture accelerating asphalt aging and the degradation of moisture susceptibility is still ambiguous. Hence, it is of great significance to understand the physicochemical effects of moisture on asphalt during immersion.

It is believed that asphalt oxidation, dissolution and migration affect the physicochemical properties during immersion. Asphalt oxidation is a kind chemical between asphalt components and oxygen, which cause pavement performance degradation [14]. The process in which some components of asphalt mix with aqueous solution to form a homogeneous phase in a molecular state is asphalt dissolution [15]. Asphalt migration means that some components of asphalt separate from the asphalt surface into aqueous solutions [16].

Noguera et al. [17] observed that the physical changes of asphalt immersed in distilled water were induced by chemical

* Corresponding author.

E-mail address: s.xu-1@tudelft.nl (S. Xu).

reactions. As a result, the aromatic/saturated ratios and resins/asphaltenes ratios of asphalt decreased, indicating that asphalt can react with oxygen molecules from the water leading to asphalt oxidation. Menapace and Masad [18] compared the effects of the aging mode with and without moisture on the asphalt by the degree of oxidation. It was found that the presence of moisture could cause the dissolution of water-soluble components of asphalt and the separation of part of asphalt from the surface. Dos Santos et al. [19] and Nivedya et al. [20] used atomic force microscopy (AFM) to study the effect of moisture on the surface structure of asphalt. The results showed that the surface structure cracked and the material leak through the cracks, causing the surface to become rougher. This means that there exists a migration of substance during immersion. Hung et al. [21] investigated the effects of high temperature or prolonged exposure to water on the asphalt by Fourier transform infrared spectroscopy (FTIR). After water exposure, the polar compounds of asphalt surface increased. Gong et al. [22] used AFM and FTIR to investigate the effect of moisture on asphalt micro properties. The interactions between moisture molecules and polar components alter the components of asphalt surface thus influencing the adhesive force. Through pull-off test for bond strength, Yang et al. [23] observed that the aggregate with 10% moisture might decrease the adhesion between asphalt and aggregate to 50% compared with the dry aggregate condition. Over time, moisture can diffuse into asphalt, reducing the adhesion between asphalt and aggregate, even causing further moisture erosion such as the increase of asphalt moisture sensitivity [24]. The researches above showed the occurrence of oxidation, dissolution and migration of asphalt and the changes of asphalt properties during immersion. However, the relevant factors of physicochemical changes of asphalt during immersion are ambiguous, so are the mechanisms.

Asphalt pavement in different area may be exposed to different kinds of aqueous solution. Due to the destruction of the atmosphere and vegetation, the rainfall pH can usually be as low as 3 in some areas of acid rain, while the pH of the soil can be up to 11 in some saline-alkali areas [25,26]. The pH of solution can largely affect the physicochemical properties of asphalt and aggregate to destroy the pavement performance [27–29]. Salt fog usually is generated by the evaporation of seawater in coastal areas and snowmelt salt is generally used on asphalt pavement in winter, which might include around 10% sodium chloride or 10% sodium sulfate [30,31]. The intrusion of saline solution can lead to chemical erosion and crystalline destruction on asphalt binder [32]. Moreover, the chemical composition of the water-soluble substance of asphalt and the interaction between aqueous solution and asphalt are still unclear. In order to improve the moisture susceptibility of asphalt to reduce the pavement distresses, it is very crucial to understand the erosion mechanism of different solutions on asphalt and the physicochemical changes of asphalt.

In view of the above background, this study investigated the erosion behaviors of five different aqueous solutions on the asphalt, including distilled water, pH 3 acid solution, pH 11 alkali solution, 10 wt% NaCl saline solution and 10 wt% Na₂SO₄ saline solution. Combining with physicochemical analysis of asphalt and residual solution, the study investigated the related erosion mechanism of different aqueous solutions on asphalt and the physicochemical changes of asphalt.

2. Materials and experiments

2.1. Materials

The asphalt binder with Pen 60/80 (simply refer to as 70A) obtained from Ezhou Kepai Asphaltic Products Co., Ltd (Hu Bei,

China) was employed in this study. The physical properties of virgin asphalt are shown in Table 1.

2.2. Experiments

2.2.1. Experiment plan

The methodology of this study was shown in Fig. 1. First, the asphalt samples were obtained by immersion in five kinds of solutions at 60 °C, including distilled water, pH 3 acid solution, pH 11 alkali solution, 10 wt% NaCl saline solution and 10 wt% Na₂SO₄ saline solution. To distinguish the effects of thermal oxygen aging, 70A was processed under the same condition without aqueous solution immersion to obtain the control samples. Then, the asphalt samples were characterized by AFM, FTIR and thin-layer chromatography with flame ionization detection (TLC-FID) test to investigate the physicochemical properties of asphalt during oxidation, dissolution and migration. Then, the residual solution after immersing the asphalt was monitored by a pH meter, total organic carbon (TOC) analyzer and FTIR to investigate the changes in the chemical properties of asphalt caused by dissolution and migration of asphalt. And the substances that dissolved and migrated from the asphalt into aqueous solution were studied after immersion. Finally, the related mechanism of moisture erosion was discussed by combining with the test results of asphalt and residual solution.

2.2.2. Immersion test

The immersion test aimed to simulate asphalt immersed in the real atmosphere. First, 5 g heated 70 A was poured into a glass dish with a diameter of 90 mm, cleaned with isopropanol to reduce the risk of microbial growth on the asphalt. The glass dish was placed in a vacuum drying box at 120 °C for 0.5 h. After cooling, a 0.78 mm asphalt film was prepared. The pH 3 acid solution was prepared with pure sulfuric acid and nitric acid, and the molar ratio of which was 9:1. The pH 11 alkali solution was obtained by dissolving solid sodium hydroxide. The pH value of the two kinds of solutions is controlled by a pH meter. And two kinds of saline solution were prepared by dissolving solid sodium chloride and solid sodium sulfate with a mass percentage of 10, respectively. Then 40 ml of each solution, including distilled water, pH 3 acid solution, pH 11 alkali solution, 10 wt% NaCl saline solution and 10 wt% Na₂SO₄ saline solution, were poured into the glass dish respectively, which made the asphalt film immersed completely. It is known that the pavement temperature in summer can reach 60 °C in most cases. To simulate solution immersion in the real atmosphere in summer, the experimental temperature of immersion test was set at 60 °C, and the experimental time was 2 days, 4 days, 6 days, 8 days and 10 days, respectively. After immersion, the asphalt films were slowly cleaned by distilled water for 5 min to wash off the saline and other water-soluble substance attached to the surface, and then placed in an oven at 110 °C for 15 min to remove moisture on the asphalt surface. The control samples were heated under the same condition without immersion to distinguish between the erosion of moisture and the effect of temperature during immersion. Then 10 ml trichloroethylene organic solvent was poured into the glass dish to dissolve the surface of asphalt films, and asphalt solution was placed in a fume cupboard for 72 h to allow trichloroethylene to evaporate completely. Finally, asphalt

Table 1
Physical properties of 70 A.

Physical properties	Unit	70A	Standards
Penetration (100 g, 5 s, 25 °C)	0.1 mm	71.6	ASTM D-5 [33]
Softening point	°C	48.3	ASTM D-36 [34]
Ductility (5 cm/min, 15 °C)	cm	> 100	ASTM D-113 [35]
Solubility (Trichloroethylene)	%	99.5	ASTM D-2042 [36]

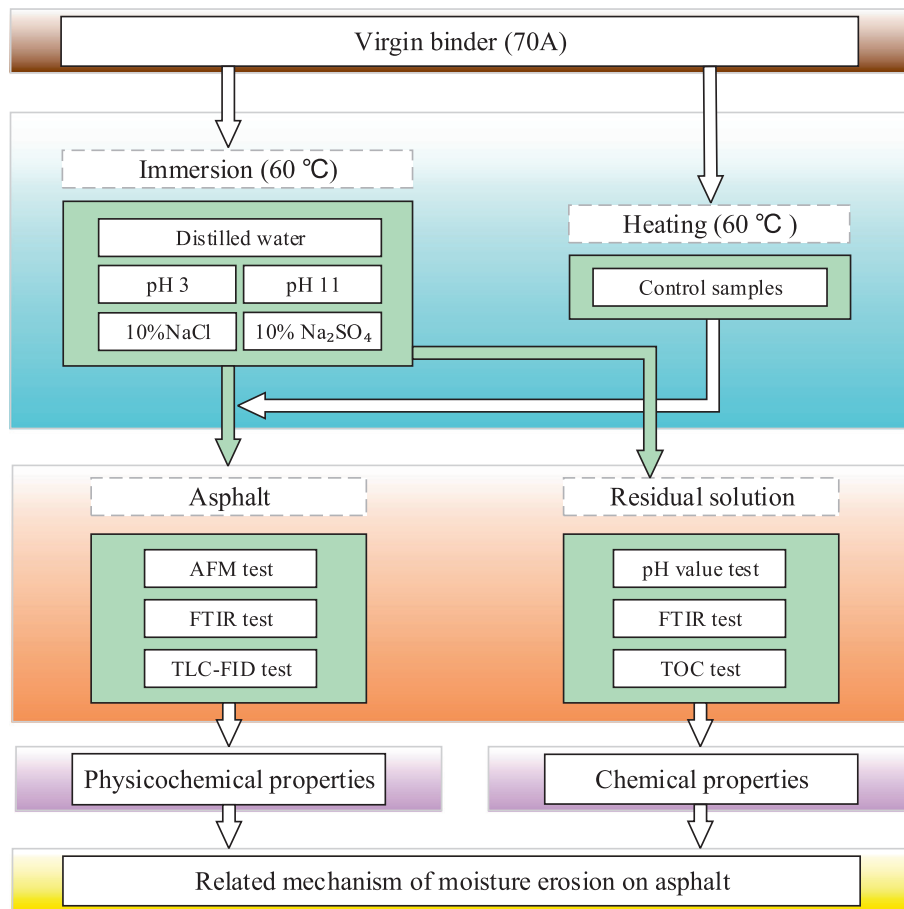


Fig. 1. The methodology of this study.

films with a thickness of 0.2 mm were obtained for AFM test and TLC-FID test. The different preparation method of asphalt samples for FTIR test was described in the characterization section of asphalt.

2.2.3. Characterization of asphalt

AFM (Nanoscope IV, DI Nanoscope TVti with Nanoscope software, American Veeco Company), FTIR (Nicolet 6700, Thermo Fisher Scientific, Waltham, MA, USA) and TLC-FID (Iatroscan MK-6, Iatron Laboratories Inc., Tokyo, Japan) were employed to investigate the microscopic changes of asphalt during immersion. After immersion, the microstructure of samples was detected by AFM in tapping mode with TAP-300 silicon cantilever tips. A drop of liquid asphalt heated to 130 °C was placed on a glass slide and then cooled to room temperature for AFM test. An etched silicon probe was applied to scan the height and Z-images of asphalt samples. The test conditions were that the elastic coefficient was 6 N/m, resonance frequency was 150 kHz and the scanning area was $20 \times 20 \mu\text{m}$. To quantitatively evaluate the bee structure (BS) of asphalt micro-surface, the two-dimensional images were processed by Matlab software. The grayscale, equalization and binarization were processed, as shown in Fig. 2. The BS called catana phase distributed unevenly that was surrounded by the dispersed phase called peri phase adjacent to the continuous phase called para phase [37]. After binarization, the image is black and white, and the white area shows the hills of BS. It clearly showed the amount and area of BS.

AFM offline software, Image-Pro Plus, was used to calculate the characteristic parameters of BS [38,39]. And the parameters and

the calculation formulas were shown in Table 2. Where the total area of sample is $400 \mu\text{m}^2$; N expresses the total number of test points.

The chemical structure of asphalt was monitored by FTIR with Omnic 6.2 software after immersion for different time. The traditional method of sample preparation is to immerse asphalt in a container, then dissolve the upper asphalt with an organic solvent such as trichloroethylene and finally drop the asphalt solution on the KBr chip for the test. However, the more experimental steps, the greater the experimental error. A new sample preparation method was adopted to avoid the error in this study. In detail, 10 wt% asphalt was added to the CS_2 solution, then 3 drops of which were dropped on the CaF_2 chip. The dried samples were immersed in aqueous solution at 60 °C. After immersion, the samples were dried directly for FTIR test, which reduced the secondary processing steps such as dissolution in the traditional sample preparation method to reduce the experimental error. The test conditions were that the range of scan wave number was from 4000 cm^{-1} to 400 cm^{-1} and the scan time was 64 times. The oxidation characteristic functional groups of asphalt were characterized by the carbonyl index ($I_{C=O}$) and sulfoxide index ($I_{S=O}$) [40]. Due to the use of CaF_2 chip, the peaks between 700 cm^{-1} and 400 cm^{-1} were messy peaks, the indexes were calculated with the following equations:

$$I_{C=O} = \frac{\text{Area of the carbonyl band centered around } 1700\text{cm}^{-1}}{\text{Area of the spectral bands between } 2000 \text{ and } 700\text{cm}^{-1}} \times 100\% \quad (1)$$

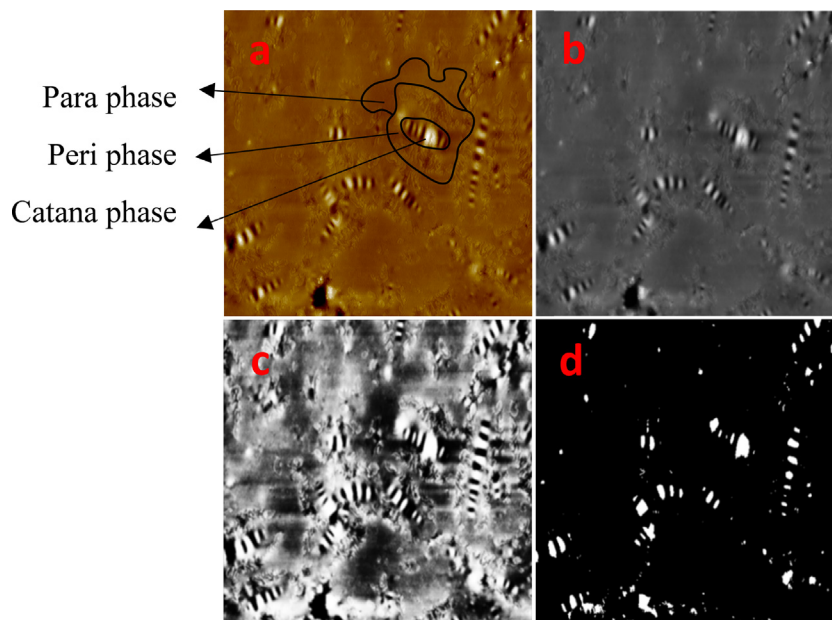


Fig. 2. Image processing of two-dimensional image (a, Virgin; b, Grayscale; c, Equalization; d, Binarization).

Table 2
Characteristic parameters of BS.

Parameter	Unit	Definition	Calculation formula
Ratio of total area (R_t)	%	Percentage of area of all BS in sample area	$R_t = \frac{\text{Total area of BS}}{\text{Total area of sample}} \times 100\%$
Ratio of single area (R_s)	%	Percentage of area of single BS in sample area	$R_s = \frac{R_t}{\text{Amount of BS}} \times 100\%$
Area of single (A_s)	μm^2	Area of single BS	$A_s = \frac{\text{Total area of BS}}{\text{Amount of BS}}$
Maximum peak (Z_p)	nm	Height of the highest peak	Z_{max}
Maximum depth of valley (Z_v)	nm	Height of the deepest valley	Z_{min}
Mean roughness (R_a)	nm	Arithmetic mean deviation of the entire three-dimensional surface	$R_a = \frac{1}{N} \sum_{i=1}^N Z_p + Z_v $

$$I_{S=0} = \frac{\text{Area of the sulphoxide band centered around } 1030\text{cm}^{-1}}{\text{Area of the spectral bands between } 2000 \text{ and } 700\text{cm}^{-1}} \times 100\% \quad (2)$$

TLC-FID test was undertaken for analyzing the four components change of asphalt with the prolongation of immersion time. The asphalt solution with 2 wt% concentration was prepared with dichloromethane and then was placed on a chromatographic column. Three kinds of organic solvent, including n-heptane, n-heptane/toluene mixture (volume ratio is 1:4) and toluene/anhydrous ethanol mixture (volume ratio is 11:9), were used as extenders to separate the four components of asphalt. Firstly, the chromatographic column was placed in a container containing 70 ml n-heptane until the asphalt solution expanded to 100 mm. Then the chromatographic column was heated at 80 °C for 60 s to remove the residual solvents. Similarly, the asphalt solution in chromatographic column expands to 50 mm and 25 mm in the container containing 70 ml n-heptane/toluene mixture and 70 ml toluene/anhydrous ethanol mixture, respectively. Finally, the data

was recorded by TLC-FID analyzer. Colloid instability index (CII) was used to characterize the colloid structure of asphalt [41] which were calculated with the content of each component as follow:

$$CII = \frac{\text{Asphaltene} + \text{Saturate}}{\text{Resin} + \text{Aromatic}} \quad (3)$$

2.2.4. Characterization of residual solution

After immersion, the changes of residual solution were detected by a pH meter (OHAUS Starter 2100, Shanghai, China), TOC analyzer (Multi-N/C2100S, Jena, German) and FTIR (Nicolet 6700, Thermo Fisher Scientific, Waltham, MA, USA) respectively. The pH meter was applied to detect the pH value of the solution after immersing asphalt for different time. The test range was from 0.00 to 14.00, and the precision was 0.01. Due to the low concentration of the organic substance, the residual solutions need to be treated for the reliability of data before FTIR test. In view of this, carbon tetrachloride was selected as the extractant to extract organics of the solution. The residual solution was poured into a separating funnel and 10 ml carbon tetrachloride was added. The separating funnel was shaken to make them blended, and then stood uprightly for 5 mins until the solution was completely stratified. Finally, the purified residual solution was collected from the lower outlet. The composition of the residual solution was observed by FTIR. Two drops of the extracted solution were dripped on a KBr chip and dried under the warm light for the test. The test conditions were the same as that of the asphalt. The TOC of the residual solution was counted to characterize the carbon migration of asphalt by combustion method TOC analyzer.

3. Results and discussions

3.1. Changes of asphalt caused by aqueous solution corrosion

3.1.1. Changes in morphology

It is believed that asphalt morphology is closely related to the chemical composition, and the distribution of four components in a single BS is shown in Fig. 3. The lighter the color, the higher the altitude. And the yellow convex area is resins; the main component of white convex area is asphaltenes; the black subsidence

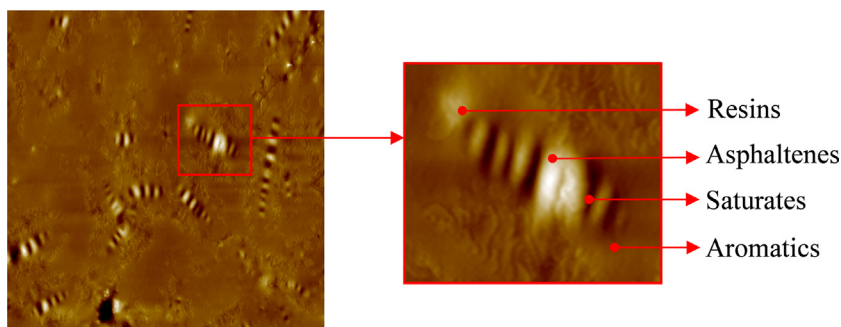


Fig. 3. Distribution of four components in a single BS.

area is saturates; and the surrounding horizontal area is aromatics [42]. The two-dimensional and three-dimensional AFM images were used to characterize the morphology of asphalt samples after immersion for 10 days, as shown in Table 3. From the two-dimensional images, compared with the control sample, the area of BS increased significantly after immersion. The asphaltenes are the main component of the convex part of BS [43]. The larger the BS, and the more the asphaltenes. Asphalt oxidation can increase the number or size of BS [44]. Thus, it indicated that asphalt oxidation might occur and cause the growth of asphaltenes. From the three-dimensional images, there were the periodically undulating hills and valleys that formed the BS. After immersion, the area of hills and valleys increased and the surface became rougher.

To quantify the influence of solutions on the BS, the binarization images were processed by Image-Pro Plus software to calculate the characteristic parameters of BS, as shown in Fig. 4. The results showed that the amount decreased after immersion in distilled water and saline solution, while the amount increased after immersion in acid solution and alkali solution. Moreover, the R_t , R_s and A_s increased after immersion. And the degree of change is greater in acid solution and alkali solution. This indicated that asphaltenes were more after immersion in acid solution and alkali solution. Thus, the constituent components of asphalt were more sensitive to pH rather than saline. It might be the interaction between them and the acid and alkali solution resulted in the more serious erosion.

From three-dimensional images, the increased of hills and valleys roughened the surface. The R_a of asphalt was used to quantify the erosion effect of aqueous solutions on the asphalt surface, as shown in Fig. 5. The R_a increased after immersion. However, Yi et al [38] observed that the R_a of asphalt decreased after oxidation aging, including ultraviolet aging and thermal oxygen aging. Thus, it might be that the aqueous solution penetrated the asphalt, leading to the increase of R_a [39]. That indicated that asphalt might be affected by dissolution and migration in addition to oxidation under the action of aqueous solution. In general, the simultaneous occurrence of oxidation, dissolution and migration of asphalt increased the R_a during immersion.

3.1.2. Changes in chemical structure

To explore the reasons for the change of asphalt morphology, the chemical structure of asphalt samples was tested by FTIR, as shown in Fig. 6. The absorption peaks at 1700 cm^{-1} and 1030 cm^{-1} were caused by the carbonyl group and sulfoxide group, both of which were the oxidation products of asphalt [45]. It could be seen that the peaks of carbonyl and sulfoxide increased with the extension of time which meant that oxidation of asphalt occurred.

To quantify the degree of oxidation, the $I_{C=O}$ and $I_{S=O}$ were compared, as shown in Fig. 7. As the main product of asphalt oxidation, the $I_{C=O}$ of all asphalt samples increased, as shown in Fig. 7a. For the

same time, the control sample has the lowest $I_{C=O}$, followed by the asphalt immersed by distilled water, Na_2SO_4 solution, NaCl solution, pH 3 solution and pH 11 solution. It indicated that the aqueous solution largely affected asphalt erosion. And solute could accelerate the oxidation of asphalt during immersion. Among them, the oxidation of asphalt occurred slowly through the reaction with oxygen in distilled water. However, the $I_{C=O}$ of asphalt immersed in pH 3 solution increased rapidly after 2 days, so did that of asphalt immersed in pH 11 solution. This could be explained by the dissolution and migration rate of polar molecules on asphalt surface increased under the action of solutes such as acid and alkali, which might promote the penetration rate of aqueous solution into the asphalt. Moreover, the presence of saline further intensified the emulsification of asphalt. It was the presence of chlorine ions that accelerated the oxidation of asphalt after immersion in NaCl saline solution [46]. When sodium sulfate intruded into the asphalt, it crystallized and expanded, increasing the porosity to accelerate the oxidation of asphalt [47].

In Fig. 7b, the $I_{S=O}$ increased rapidly after immersion. And sulfuric acid and mercaptan compounds of asphalt undergone oxidation condensation reaction to form subacid compounds and disulfide during immersion in pH 3 acid solution, causing a sharp increase of $I_{S=O}$ [48]. The results further proved that the solute could accelerate the asphalt oxidation, and the effect increased in the following order, Na_2SO_4 saline < NaCl saline < pH 3 acid < pH 11 alkali.

3.1.3. Changes in constituent components

Like the formation of carbonyl and sulfoxide functional groups, the increase of asphaltenes has also been widely recognized as oxidation indicators of asphalt [49]. The four components of all asphalt samples were measured by TLC-FID after immersion for different time, as shown in Fig. 8. After heating for 10 days, the saturates and aromatics of control sample decreased by 3.23% and 1.62%, respectively; whereas the resins and asphaltenes increased by 2.32% and 6.97%, respectively. This was the result of asphalt thermal oxygen aging. After immersion for 10 days, the saturates, aromatics and resins of asphalt immersed in distilled water decreased by 3.54%, 1.82% and 1.25%, respectively; whereas the asphaltenes increased by 11.58%. It indicated that asphalt dissolution and migration occurred during immersion, resulting in the decrease of resins. The aromatics and resins of asphalt immersed in pH 3 solution decreased by 0.04% and 25.27%, respectively; whereas the saturates and asphaltenes increased by 5.31% and 18.79%, respectively. It was probably because the esterification reaction between olefin of asphalt and sulfuric acid formed sulfites or sulfates. Then the cationic intermediate that was formed by the reaction between them and isomeric alkane reacted with olefin of asphalt to form long-chain isomeric alkane, which increased the content of saturates [48]. The saturates, aromatics and resins of asphalt soaked in pH 11 solution decreased by 3.28%, 1.98% and

Table 3
AFM images of asphalt after immersion for 10 days.

Sample	Two-dimensional image	Three-dimensional image
Control		
Distilled water		
pH 3		
pH 11		
NaCl		
Na ₂ SO ₄		

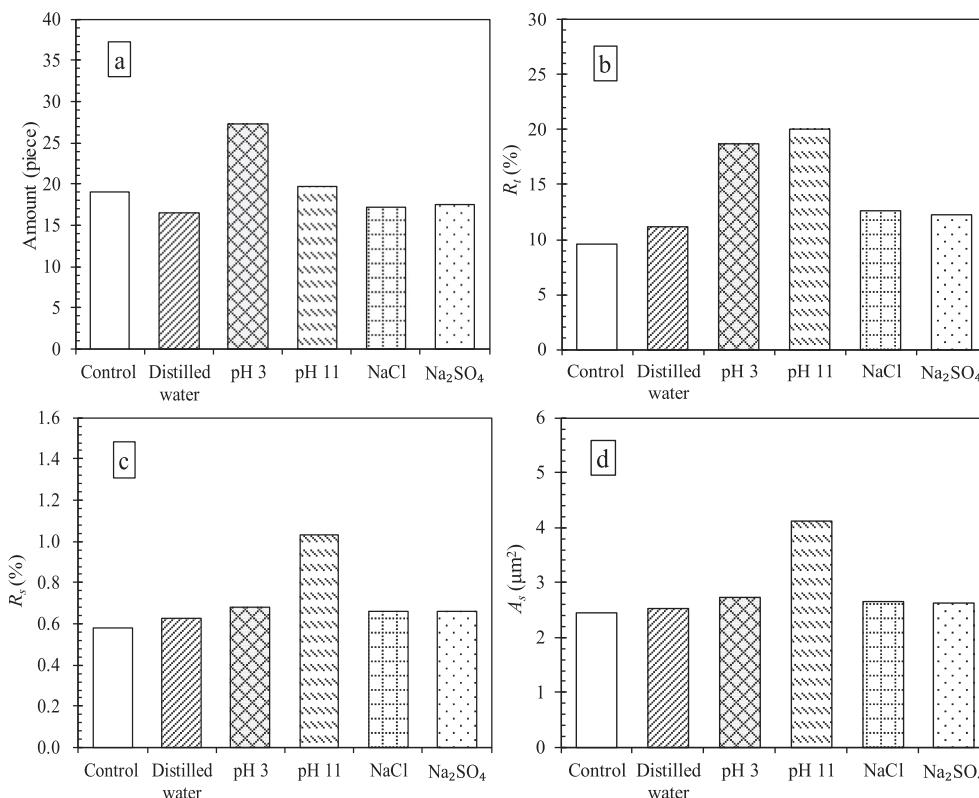


Fig. 4. Parameters of BS on asphalt micro-surface after immersion for 10 days (a. Amount; b. R_1 ; c. R_2 ; d. A_s).

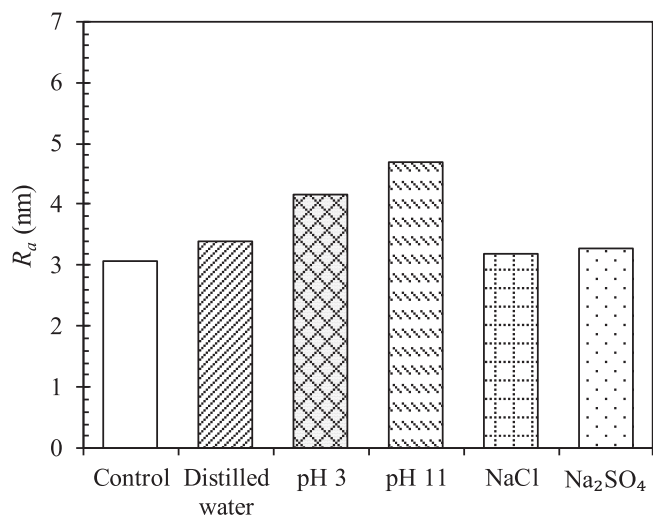


Fig. 5. R_a of asphalt after immersion for 10 days.

33.71%, respectively; while the asphaltenes increased by 44.27%. NaOH might react with the fatty acids in resins to form small molecule products, resulting in the sharp reduction of resins during immersion in pH 11 solution [50]. The saturates, aromatics and resins of asphalt after immersed in NaCl solution decreased by 1.87%, 1.72% and 5.47%, respectively; while the asphaltenes increased by 13.40%. The saturates, aromatics and resins of asphalt after immersed in Na_2SO_4 solution decreased by 1.35%, 0.48% and 8.98%, respectively; whereas the asphaltenes increased by 12.23%. The asphaltenes of asphalt immersed in two kinds of saline solution were more than that of asphalt immersed in distilled

water. The presence of saline caused the chemical erosion on asphalt during immersion.

In general, the saturates and aromatics might be stripped from the asphalt surface, leading to the decreased of the content. The aromatics and resins might react with the oxygen to form the asphaltenes, leading the decrease of aromatics and resins and the increase of asphaltenes [51]. And the resins might contain water-soluble polar substances and ions, and they were more hydrophilic in aqueous solutions than that of other components, such as the dissolution and ionization of carboxylic acids and phenols, causing the resins to continue to decrease with time [15]. Among them, the saturates and aromatics of all samples increased while the resins and asphaltenes decreased after immersion for 4 days, which might be due to the dissolution of the water-soluble substances of resins and asphaltenes. Over time, the asphaltenes of all asphalt samples began to increase, indicating that the oxidation reaction of aromatics and resins was dominant.

The CII was compared to study the influence of solute on the colloid structure of asphalt, as shown in Fig. 9. After heating for 10 days, the CII of control asphalt increased by 2.01%. The thermal oxygen aging changed the colloid structure of asphalt from sol to gel structure. After immersion in distilled water, pH 3 acid solution, pH 11 alkali solution, NaCl saline solution and Na_2SO_4 saline solution for 10 days, the CII of asphalt increased by 4.95%, 28.39%, 30.18%, 7.72% and 6.38%, respectively. It indicated that the erosion of aqueous solution could also change the colloid structure of asphalt from sol to gel structure. And the addition of solute, including acid, alkali and saline, increased the colloidal instability index of asphalt, and the influence degree increased in the following order, Na_2SO_4 saline < NaCl saline < pH 3 acid < pH 11 alkali. With the growing of time, these solutes had a more significant promoting effect on asphalt aging. The results are consistent with the above analysis results of FTIR test.

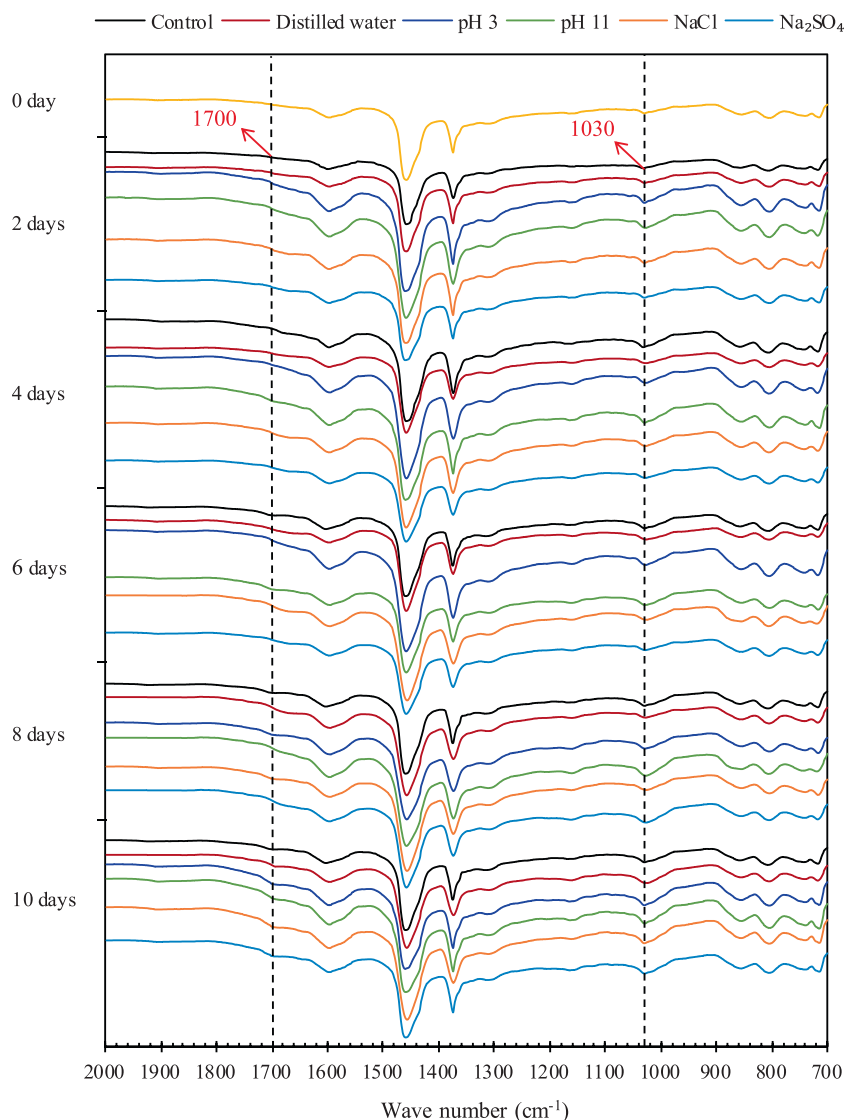


Fig. 6. The FTIR spectrum of asphalt after immersion.

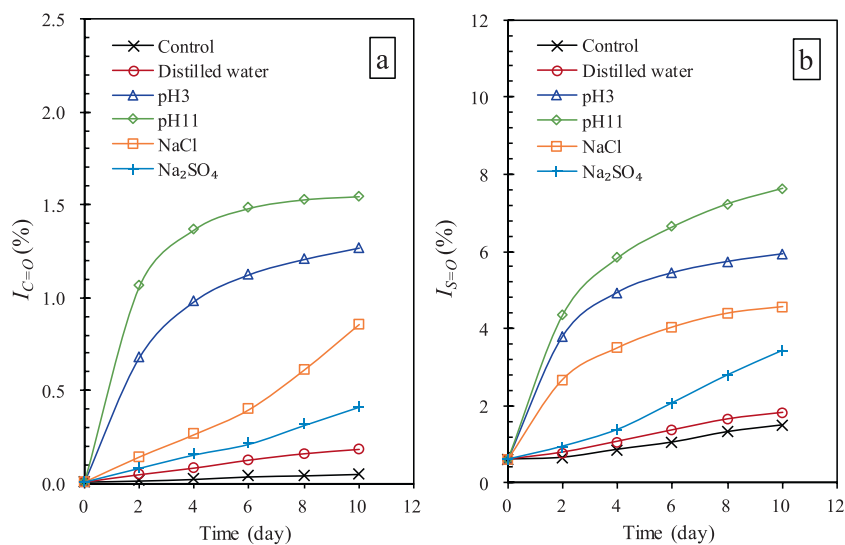


Fig. 7. $I_{C=O}$ and $I_{S=O}$ of asphalt after immersion (a. $I_{C=O}$; b. $I_{S=O}$).

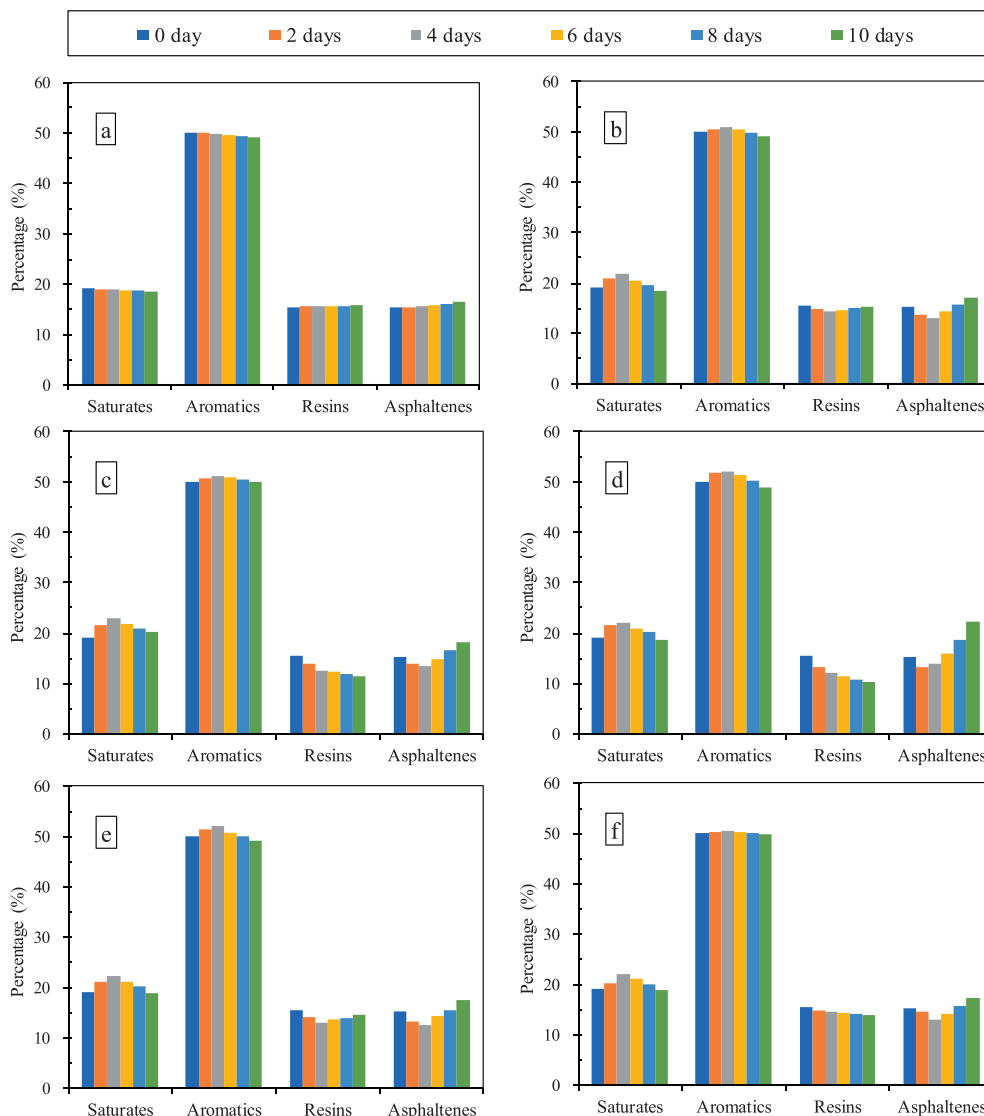


Fig. 8. Four components of asphalt after immersion for different time (a. Control; b. Distilled water; c. pH 3; d. pH 11; e. NaCl; f. Na_2SO_4).

3.2. Changes in aqueous solution after immersing asphalt

3.2.1. Changes in pH value

To better understand the change in physicochemical properties of asphalt during immersion in different aqueous solution, the pH value of the residual solution was observed after soaking asphalt samples, as shown in Fig. 10. It could be found that the pH value of all residual solution decreased, in addition to the pH 3 acid solution. The distilled water gradually became acid, manifesting that the most of soluble substances of asphalt were acid. However, the pH value of pH 3 acid solution increased with the extension of time. It was on account of sulfuric acid that could react with the olefins of asphalt, reducing the concentration of hydrogen ions in the solution. After immersion for 10 days, the pH 11 alkali solution performed the greatest change of pH value, which was as low as 7.00. This could be explained by the fact that alkali could react with the active component of asphalt to form soaps and fatty acids, accelerating the neutralization of alkali [50]. Saline solutions such as NaCl and Na_2SO_4 had higher surface energy and were more likely to intrude into asphalt film than distilled water, increasing dissolution and migration [52]. Hence, it was inferred that some substances of asphalt dissolved and migrated under the action of

the solution and most of them were acid. There were not only physical changes but also chemical reactions during the immersion.

3.2.2. Changes in chemical components

FTIR was applied to investigate the substances dissolved and migrated from asphalt into the aqueous solution, as shown in Fig. 11. Apparently, the characteristic absorption peaks corresponding to different solute aqueous solutions were approximately the same. Through specific analysis of peaks in the infrared spectrum, there were 14 kinds of characteristic absorption bands in the wavenumber range of $4000 \sim 400 \text{ cm}^{-1}$, as shown in Table 4. It could be seen that alkanes, aromatic hydrocarbons, sulfoxides, amines, amides, carboxylic acids and ethers might exist in the residual solutions. Among them, the alkanes and aromatic hydrocarbons existed because of the migration of light components, such as saturates and aromatics. And sulfoxides, amides, carboxylic acid and esters were the product of asphalt oxidation [53]. The pH value test results indicated that most of substances dissolved and migrated from asphalt were acid. Amines and amides are alkaline but carboxylic acids are acid, so the content of carboxylic acids in all residual solutions is greater than that of amines and amides

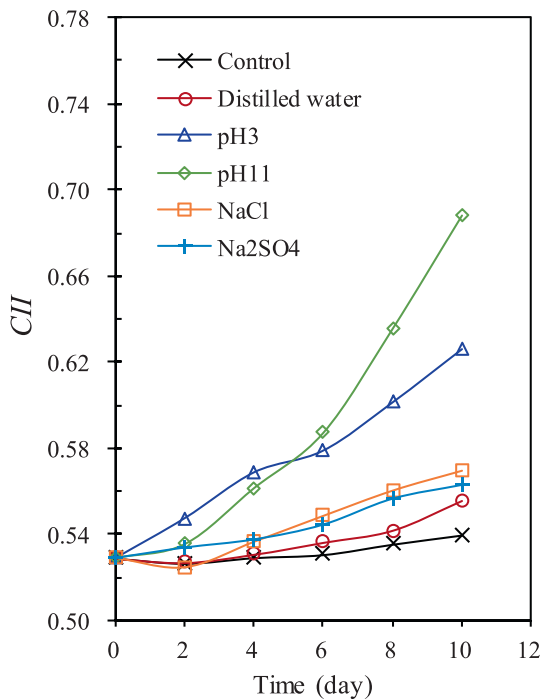


Fig. 9. CII of asphalt after immersion.

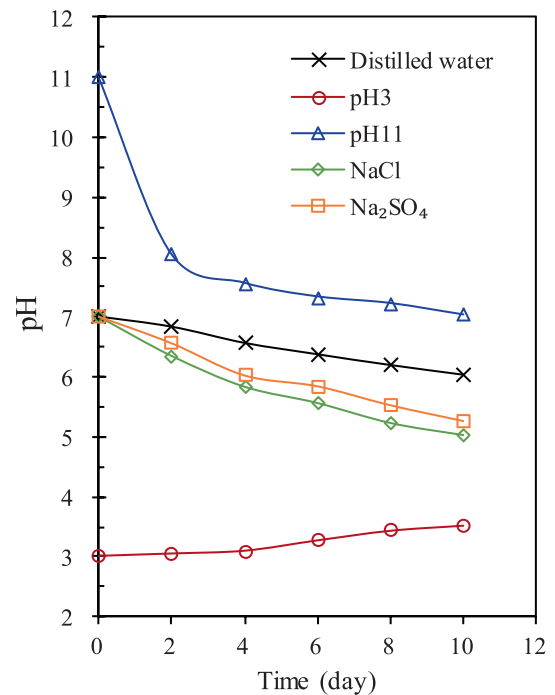


Fig. 10. pH changes of aqueous solution with immersion time.

except for alkali solution. NaOH might be gradually neutralized by carboxylic acids migrated from asphalt into pH 11 alkali solution, so the pH value gradually approached 7. In general, partial components and oxidation product of asphalt dissolved and migrated into solution because of physical erosion and chemical reactions.

3.2.3. Changes in TOC

To quantify the substances dissolved and migrated from asphalt, TOC analyzer was undertaken for counting the TOC of the residual solution to verify the erosion degree of the five kinds of solutions on asphalt, as shown in Fig. 12. It can be seen that

the TOC increased after immersion, indicating that some organic substances of asphalt dissolved and migrated into the aqueous solution. With immersion time, the TOC gradually increased, which means that the erosion degree of aqueous solution on asphalt increased over time. After immersion for 10 days, the TOC of different residual solutions increased in the following order, distilled water < Na₂SO₄ saline solution < NaCl saline solution < pH 3 acid solution < pH 11 alkali solution. Distilled water had the lowest the TOC, but it wasn't zero. That means there existed some soluble substances of asphalt, which is consistent with the above results of the pH value test. The relationship between TOC and immersion

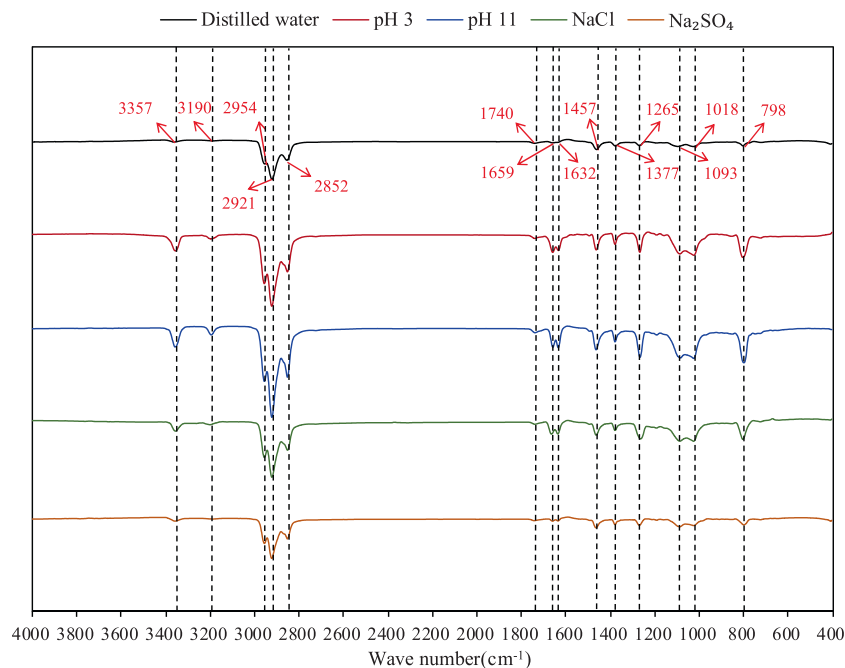


Fig. 11. The infrared spectrum of residual solution after immersion for 10 days.

Table 4
The absorption bands of the residual solution.

Wavenumber (cm ⁻¹)	Functional group	Wavenumber (cm ⁻¹)	Functional group
3357	Stretching vibration of N-H in amine	1632	Stretching vibration of C = O or bending vibration of N-H in amide
3190	Stretching vibration of C-H in amine	1457	Scissoring vibration of C-H in -CH ₂ - or -CH ₃
2954	Asymmetrical stretching vibration of C-H in -CH ₃	1377	Bending vibration of C-H in -CH ₂ - or -CH ₃
2921	Asymmetric stretching vibration of C-H in -CH ₂ -	1265	Stretching vibration of C-O in carboxylic acid or aromatic oxide
2852	Symmetric stretching vibration of C-H in -CH ₂ -	1093	Stretching vibration of C-O in aliphatic ether
1740	Stretching vibration of C = O in carboxylic acid	1018	Stretching vibration of S = O
1659	Stretching vibration of C = O in amide	798	Out-of-plane bending vibration of N-H in amide

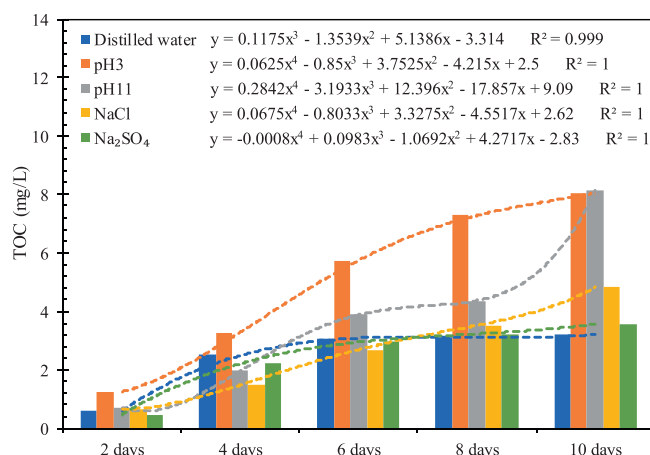


Fig. 12. TOC of the residual solution after immersion.

time could be described by the resulting polynomial regression equations, the correlation coefficients R^2 of which were all over 0.99. The TOC of residual solution can be predicted by these equations based on immersion. And it can be predicted from the trend line that the TOC of alkali solution will increase sharply after more than 10 days. These substances that dissolved and migrated from asphalt are more sensitive to alkali solution. The interaction between aqueous solution and asphalt aggravated the dissolution and migration of asphalt. The more the substances dissolved and migrated from asphalt, the more serious the corrosion. That could result in the thinning of asphalt film and further deterioration of the asphalt concrete performance [54].

4. Conclusions

In this study, the effect of different aqueous solutions on the physicochemical properties of asphalt was investigated from the perspectives of oxidation, dissolution and migration of asphalt.

Five kinds of solutions were used for asphalt immersion treatment. And AFM, FTIR, TLC-FID, pH value and TOC test methods were applied to monitor the asphalt and residual solution after immersion, respectively. The following conclusions can be drawn:

- Based on the test results of asphalt, oxidation, dissolution and migration of asphalt occurred alternately. And the dissolution and migration were dominant first, and then the oxidation was dominant over time. The erosion of aqueous solution could change the BS on asphalt microstructure and increased the R_a . And the oxidation indicators such as $I_{C=O}$, $I_{S=O}$ and asphaltenes increased after immersion because the interaction between aqueous solution and asphalt accelerated asphalt oxidation and changed the colloid structure of asphalt from sol to gel structure.
- The majority of substances dissolved and migrated from asphalt were acid, including alkanes, aromatic hydrocarbons, sulfoxides, amines, amides, carboxylic acids and ethers.
- Combining with the test results of asphalt and residual solution, it could be found that there was not only physical erosion but also chemical reactions during immersion in different aqueous solution. And solute could accelerate the moisture erosion on the asphalt through interaction, the degree of which increased in the following order, Na₂SO₄ saline < NaCl saline < pH 3 acid < pH 11 alkali.

CRedit authorship contribution statement

Yingxue Zou: Investigation, Methodology, Writing - original draft. **Serji Amirkhani:** Conceptualization, Formal analysis. **Shi Xu:** Writing - review & editing. **Yuanyuan Li:** Software, Methodology. **Yafei Wang:** Data curation, Investigation. **Jianwei Zhang:** Writing - review & editing.

Declaration of Competing Interest

The authors declare that they have no known competing financial interests or personal relationships that could have appeared to influence the work reported in this paper.

Acknowledgement

This research was supported by National Key R&D Program of China (No. 2017YFE0111600), Technological Innovation Major Project of Hubei Province (2019ACA147, 2019AEE023) and National Natural Science Foundation of China (No. 51778515).

References

- [1] H.R. Hmoud, Evaluation of VMA and film thickness requirements in hot-mix asphalt, *Mod. Appl. Sci.* 5 (4) (2011) 166–176.
- [2] M. Faramarzi, B. Golestani, K.W. Lee, Improving moisture sensitivity and mechanical properties of sulfur extended asphalt mixture by nano-antistripping agent, *Constr. Build. Mater.* 133 (2017) 534–542.
- [3] P. Chaturabong, H.U. Bahia, The evaluation of relative effect of moisture in Hamburg wheel tracking test, *Constr. Build. Mater.* 153 (2017) 337–345.
- [4] M. Guo, Y. Tan, S. Zhou, Multiscale test research on interfacial adhesion property of cold mix asphalt, *Constr. Build. Mater.* 68 (2014) 769–776.
- [5] Y. Tan, M. Guo, Using surface free energy method to study the cohesion and adhesion of asphalt mastic, *Constr. Build. Mater.* 47 (2013) 254–260.
- [6] F. Moghadas Nejad, M. Arabani, G.H. Hamed, A.R. Azarhoosh, Influence of using polymeric aggregate treatment on moisture damage in hot mix asphalt, *Constr. Build. Mater.* 47 (2013) 1523–1527.
- [7] R.A. Tarefder, M. Ahmad, Evaluating the relationship between permeability and moisture damage of asphalt concrete pavements, *J. Mater. Civ. Eng.* 27 (5) (2015) 04014172, [https://doi.org/10.1061/\(ASCE\)JMT.1943-5533.0001129](https://doi.org/10.1061/(ASCE)JMT.1943-5533.0001129).
- [8] E.H. Fini, A.M. Hung, A. Roy, Active mineral fillers arrest migrations of alkane acids to the interface of bitumen and siliceous surfaces, *ACS Sustain. Chem. Eng.* 7 (12) (2019) 10340–10348.
- [9] S. Anastasio, I. Hoff, C.C. Thodesen, H.U. Bahia, Laboratory testing methods for evaluating the moisture damage on the aggregate-asphalt system, 8th RILEM

- International Symposium on Testing and Characterization of Sustainable and Innovative Bituminous Materials, RILEM Bookseries 11 (2016) 533–543.
- [10] X. Cui, J. Zhang, N.a. Zhang, Y. Zhou, Z. Gao, W. Sui, Laboratory simulation tests of effect of mechanical damage on moisture damage evolution in hot-mix asphalt pavement, *Int. J. Pavement Eng.* 16 (8) (2015) 699–709.
 - [11] Z. Zhang, Early diseases of asphalt pavement damage of water research and countermeasures, *Applied Mechanics and Materials* 707 (2014) 532.
 - [12] L.D. Poulikakos, M.K. Tiwari, M.N. Partl, Analysis of failure mechanism of bitumen films, *Fuel* 106 (2013) 437–447.
 - [13] M. Ahmad, U.A. Mannan, M.R. Islam, R.A. Tarefder, Chemical and mechanical changes in asphalt binder due to moisture conditioning, *Road Materials & Pavement Design An International Journal* 19 (5) (2018) 1216–1229.
 - [14] W. Ye, W. Jiang, P. Li, D. Yuan, J. Shan, J. Xiao, Analysis of mechanism and time-temperature equivalent effects of asphalt binder in short-term aging, *Constr. Build. Mater.* 215 (2019) 823–838.
 - [15] L. Pang, X. Zhang, S. Wu, Y. Ye, Y. Li, Influence of water solute exposure on the chemical evolution and rheological properties of asphalt, *Materials* 11 (6) (2018) 983.
 - [16] Y.R. Song, C.X. Wang, Y.Z. Zhang, Moisture damage-component of road asphalt and its influencing factors, *Journal of China University of Petroleum* 35 (4) (2011) 172–176.
 - [17] J.A. Hernández Noguera, H.A. Rondón Quintana, W.D. Fernández Gómez, The influence of water on the oxidation of asphalt cements, *Constr. Build. Mater.* 71 (2014) 451–455.
 - [18] I. Menapace, E. Masad, The influence of moisture on the evolution of the microstructure of asphalt binders with aging, *Road Materials and Pavement Design* 21 (2) (2020) 331–346.
 - [19] S. dos Santos, M.N. Partl, L.D. Poulikakos, Newly observed effects of water on the microstructures of bitumen surface, *Constr. Build. Mater.* 71 (2014) 618–627.
 - [20] M.K. Nivedya, T.G. Trottier, X. Yu, M. Tao, N.A. Burnham, R.B. Mallick, Microstructural evolution of asphalt binder under combined action of moisture and pressure, *Journal of Transportation Engineering, Part B: Pavements* 145 (2) (2019) 06019001, <https://doi.org/10.1061/JPEODX.0000104>.
 - [21] A.M. Hung, A. Goodwin, E.H. Fini, Effects of water exposure on bitumen surface microstructure, *Constr. Build. Mater.* 135 (2017) 682–688.
 - [22] M. Gong, Z. Yao, Z. Xiong, J. Yang, J. Hong, Investigation on the influences of moisture on asphalt's micro properties by using atomic force microscopy and Fourier transform infrared spectroscopy, *Constr. Build. Mater.* 183 (2018) 171–179.
 - [23] S.-H. Yang, F. Rachman, H.A. Susanto, Effect of moisture in aggregate on adhesive properties of warm-mix asphalt, *Constr. Build. Mater.* 190 (2018) 1295–1307.
 - [24] H. Yang, L. Pang, Y. Zou, Q. Liu, J. Xie, The effect of water solution erosion on rheological, cohesion and adhesion properties of asphalt, *Constr. Build. Mater.* 246 (2020) 118465, <https://doi.org/10.1016/j.conbuildmat.2020.118465>.
 - [25] A.T. Simonović, Ž.Z. Tasić, M.B. Radovanović, M.B. Petrović Mihajlović, M.M. Antonijević, Influence of 5-chlorobenzotriazole on inhibition of copper corrosion in acid rain solution, *ACS Omega* 5 (22) (2020) 12832–12841.
 - [26] G.W.W. Wamelink, D.J.J. Walvoort, M.E. Sanders, H.A.M. Meeuwse, R.M.A. Wegman, R. Pouwels, M. Knotters, Prediction of soil pH patterns in nature areas on a national scale, *Applied Vegetation Science* (2019).
 - [27] X. Zeng, Y. Li, Y. Ran, K. Yang, F. Qu, P. Wang, Deterioration mechanism of CA mortar due to simulated acid rain, *Constr. Build. Mater.* 168 (2018) 1008–1015.
 - [28] X.J. Feng, X.u. Xiong, Corrosion effect of acid rain on the technical properties of mineral aggregates, *Adv. Mat. Res.* 690–693 (2013) 3576–3579.
 - [29] B. Shu, S. Wu, L. Dong, J. Norambuena-Contreras, Y. Li, C. Li, X.u. Yang, Q. Liu, Q. Wang, F. Wang, D.M. Barbieri, M. Yuan, S. Bao, M. Zhou, G. Zeng, Self-healing capability of asphalt mixture containing polymeric composite fibers under acid and saline-alkali water solutions, *J Clean Prod* 268 (2020) 122387, <https://doi.org/10.1016/j.jclepro.2020.122387>.
 - [30] D. Kang, Y. Yoo, J. Park, Accelerated chemical conversion of metal cations dissolved in seawater-based reject brine solution for desalination and CO₂ utilization, *Desalination* 473 (2020) 114147, <https://doi.org/10.1016/j.desal.2019.114147>.
 - [31] Z. Wang, T. Zhang, M. Shao, T. Ai, P. Zhao, Investigation on snow-melting performance of asphalt mixtures incorporating with salt-storage aggregates, *Constr. Build. Mater.* 142 (2017) 187–198.
 - [32] R. Xiong, C.i. Chu, N. Qiao, L.u. Wang, F.a. Yang, Y. Sheng, B. Guan, D. Niu, J. Geng, H. Chen, Performance evaluation of asphalt mixture exposed to dynamic water and chlorine salt erosion, *Constr. Build. Mater.* 201 (2019) 121–126.
 - [33] D. Astm, Standard test method for penetration of bituminous materials, ASTM International, USA, 2013.
 - [34] D. Astm, D36., Standard test method for softening point of bitumen (ring-and-ball apparatus), Annual Book of Standards (2009).
 - [35] ASTM, Standard test method for ductility of bituminous materials (2007).
 - [36] ASTM, Standard test method for solubility of asphalt materials in trichloroethylene, ASTM International West Conshohocken, PA (2015).
 - [37] Åsa.L. Lyne, V. Wallqvist, B. Birgisson, Adhesive surface characteristics of bitumen binders investigated by atomic force microscopy, *Fuel* 113 (2013) 248–256.
 - [38] J. Yi, X. Pang, D. Yao, X. Meng, D. Feng, Characterization of surface roughness and adhesive mechanism of asphalt and mineral aggregate based on atomic force microscopy method, *Acta Materialia Sinica* 34 (5) (2017) 1111–1121.
 - [39] X. Ji, Y. Hou, H. Zou, B. Chen, Y. Jiang, Study of surface microscopic properties of asphalt based on atomic force microscopy, *Constr. Build. Mater.* 242 (2020) 118025, <https://doi.org/10.1016/j.conbuildmat.2020.118025>.
 - [40] M. Chen, B. Leng, S. Wu, Y. Sang, Physical, chemical and rheological properties of waste edible vegetable oil rejuvenated asphalt binders, *Constr. Build. Mater.* 66 (2014) 286–298.
 - [41] R. Guzmán, J. Ancheyta, F. Trejo, S. Rodríguez, Methods for determining asphaltene stability in crude oils, *Fuel* 188 (2017) 530–543.
 - [42] H. Zhang, Y. Wang, T. Yu, Z. Liu, Microstructural characteristics of differently aged asphalt samples based on atomic force microscopy (AFM), *Constr. Build. Mater.* 255 (2020) 119388, <https://doi.org/10.1016/j.conbuildmat.2020.119388>.
 - [43] W. Ma, T. Huang, S. Guo, C. Yang, Y. Ding, C. Hu, Atomic force microscope study of the aging/rejuvenating effect on asphalt morphology and adhesion performance, *Constr. Build. Mater.* 205 (2019) 642–655.
 - [44] H. Hong, H. Zhang, S. Zhang, Effect of multi-dimensional nanomaterials on the aging behavior of asphalt by atomic force microscope, *Constr. Build. Mater.* 260 (2020) 120389, <https://doi.org/10.1016/j.conbuildmat.2020.120389>.
 - [45] Z.-gang. Feng, S.-juan. Wang, H.-juan. Bian, Q.-long. Guo, X.-jun. Li, FTIR and rheology analysis of aging on different ultraviolet absorber modified bitumens, *Constr. Build. Mater.* 115 (2016) 48–53.
 - [46] X. Zha, X. Ren, G. Fu, Influence of chlorine salt as a snowmelt agent on pavement performances for SBS modified asphalt mixtures, *Journal of Transport Science and Engineering* 1 (2012).
 - [47] Y. Wang, J. Ye, Y. Liu, X. Qiang, L. Feng, Influence of freeze–thaw cycles on properties of asphalt-modified epoxy repair materials, *Constr. Build. Mater.* 41 (2013) 580–585.
 - [48] X. Feng, A. Chen, X. Wang, X. Xiong, Research on technical performance and corrosion mechanism of asphalt corroded by acid rain, *Highway* 4 (2017) 223–228.
 - [49] S. Caro, A. Diaz, D. Rojas, H. Nuñez, A micromechanical model to evaluate the impact of air void content and connectivity in the oxidation of asphalt mixtures, *Constr. Build. Mater.* 61 (2014) 181–190.
 - [50] W. Pu, C. Shen, T. Xiangjian, B. Wei, N. Zhao, Z. Mei, Research advances about oil-water interfacial dilational viscoelasticity in chemical flooding, *Oilfield Chemistry* 03 (2018) 562–570.
 - [51] R.A. Tarefder, I. Arisa, Molecular dynamic simulations for determining change in thermodynamic properties of asphaltene and resin because of aging, *Energy Fuels* 25 (5) (2011) 2211–2222.
 - [52] D. Feng, J. Yi, D. Wang, L. Chen, Impact of salt and freeze–thaw cycles on performance of asphalt mixtures in coastal frozen region of China, *Cold Reg. Sci. Technol.* 62 (1) (2010) 34–41.
 - [53] H. Yao, Q. Dai, Z. You, Chemo-physical analysis and molecular dynamics (MD) simulation of moisture susceptibility of nano hydrated lime modified asphalt mixtures, *Constr. Build. Mater.* 101 (2015) 536–547.
 - [54] M. Dong, W. Sun, L. Li, Y. Gao, Effect of asphalt film thickness on shear mechanical properties of asphalt-aggregate interface, *Constr. Build. Mater.* 263 (2020) 120208, <https://doi.org/10.1016/j.conbuildmat.2020.120208>.